CRATER FORMATION IN THE TRANSITION FROM CIRCULAR TO ELLIPTICAL IMPACT STRUCTURES. D. Elbeshausen[1], K. Wünnemann. Museum für Naturkunde, Leibniz Institute for Research on Evolution and Biodiversity, Invalidenstr. 43, D-10115 Berlin, Germany. [1]Contact: dirk.elbeshausen@mfn-berlin.de

Introduction: The vast majority of impact craters on planetary surfaces is circular. Given that most impacts occur at an oblique angle of impact this observation implies that the overall shape of craters formed by hypervelocity impacts is not sensitive to the impact angle and direction. However, 5% of impact craters on planetary surfaces are elliptical, with an ellipticity of 1.1 or greater. The frequency of elliptical craters was found to be consistent with the assumption that impacts at or below 12° form elliptical craters [1].

Despite their rare occurance the study of elliptical craters and the gradual transition from circular to elongated crater shapes allows for a better understanding of crater formation in general. In the present study we conducted 3D hydrocode models [2,3] to investigate crater formation at highly oblique impacts. Previously [4], the code has been successfully used to reproduce the formation of elliptical craters from laboratory experiments in metal [5]. It was shown that the cohesive strength strongly influences the threshold impact angle for the formation of elliptical craters [6,7]. However, in these studies only relatively low-energy (small-scale) impacts were investigated. Here we extend the previously used parameter space by assuming a larger range of impact energies and we also vary the target material properties to investigate at which critical angle the transition from circular to elliptical impact craters occur. In particular we want to understand how the crater formation mechanism changes during the transition from circular the elliptical craters.

Hydrocode simulations: To investigate crater formation at very oblique impact angles we carried out a series of 3D simulations by using the multi-rheology hydrocode iSALE-3D [2,3]. We assumed Earth-like gravity conditions of g=9.81m/s^2 and varied the impact angle between 90° (vertical impact) and 5°, focusing on impacts below 30° where the transition from circular to elliptical craters is expected. To avoid the additional complication of material vaporization impact velocity was kept constant at a relatively low value of U=8 km/s. To study the effect of different impact energies, we varied the impactor diameter L over two orders of magnitude (500m – 5 km). The thermodynamic state of the material was computed by the Tillotson equation of state [8] using parameters for granite as stated in [9]. To study the effect of material strength, we varied both the coefficient of internal friction (f=0.2, 0.3, 0.4, and 0.7) and cohesion (Y_{coh}=0, 5, 20, 100, and 200 MPa) assuming a Drucker-Prager strength model ($Y = Y_{coh}+fP$, where P is pressure). We do not take tensile failure into account. Hence, fragmentation of the projectile is neglected in our simulations although it may be an important aspect in highly oblique impacts.

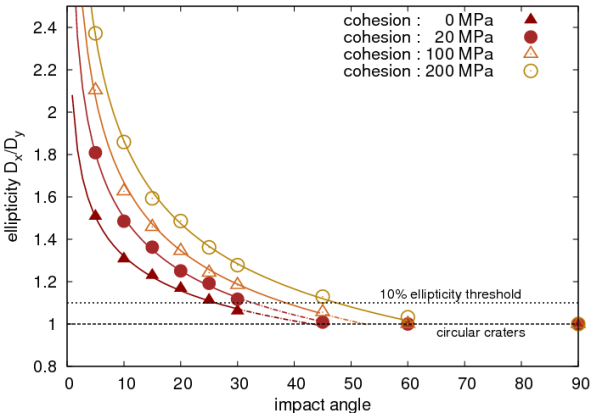

Fig. 1: Ellipticity vs. impact angle for L=500 m, f=0.7 and a varied cohesive strength.

When do elliptic craters form? Following the definition of [1], we define an elliptical crater as a crater with an ellipticity (length divided by width) of 1.1 or more. Using this definition, our study shows that vertical impacts as well as oblique impacts up to 45°-30° generate circular craters, which is in good agreement to observations on planetary surfaces. The critical angle, under which elliptical craters are formed, slightly decreases with projectile size (or impact energy). Internal friction does not affect significantly the formation of elliptical craters, whereas cohesion does, as shown in Figure 1. This is consistent with the assumption that the critical angle depends on the ratio of crater diameter to impactor diameter [1,6]. Generally speaking: The more resistant the target material is against plastic deformation, the larger the required angle of impact at which elliptical craters evolve. This implies that a planetary surface with higher strength would be covered by more elliptical craters than a body composed of weaker material (assuming the same impact rates and angle probabilities for all planetary bodies).

How do elliptical craters form? We identified three different regimes indicating the transition from circular to elliptical impact craters. For a particular strength and impact energy the regimes correspond to impact angles of 20°, 10°, and 5°, as shown in the snapshots in Fig. 2. In the ***transition regime*** (Fig. 2a: 20°) crater growth is similar to moderate oblique impacts (>30°). However, most of the ejected material moves parallel to the target surface, indicating the transition to the ***ricochet regime*** (Fig. 2b: 10°). Here, the projectile hardly penetrates into the target while it undergoes shockwave compression. Initially, crater formation is mainly driven by the momentum transfer from the projectile to target material (the projectile pushes material out of its way) and a highly elliptical crater evolves. Subsequently, the shock-induced relatively symmetric excavation flow (originating from a point source)

superimposes the initial processes, resulting in an elliptical, but still relatively deep impact crater. In the ***grazing regime*** (Fig. 2c: 5°), the projectile barely penetrates into the target. Thus, only a small portion of the impact energy is transferred into the target (see also [2]). This results in low amplitudes of the shockwaves. As visible in the color of projectile tracers in Fig. 2c (left), only a fraction of the projectiles encounters pressures in excess of 3 GPa, the Hugoniot-elastic limit typical for natural materials. Early reflections of shock and rarefaction waves in the projectile avoid plastic deformation in the upper part of the body. The strong pressure gradient in the projectile suggests the occurrence of fragmentation or even a decapitation of the projectile (see also [4,10]).

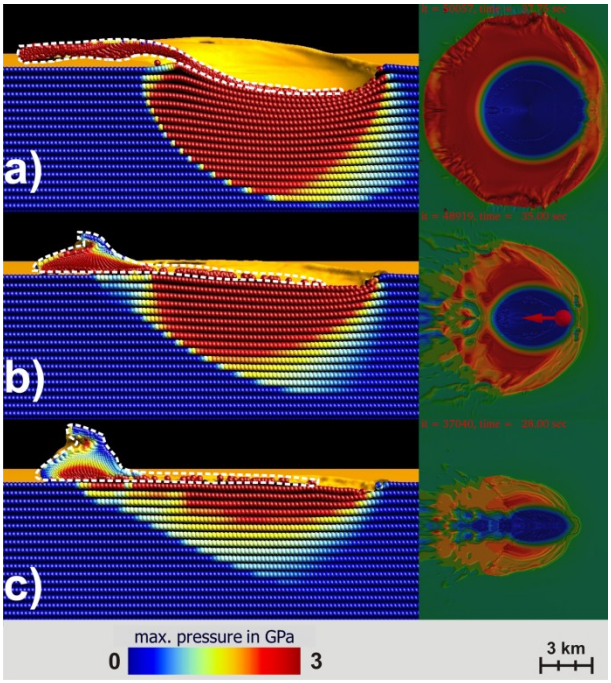

Fig. 2: Snapshots of the three regimes characterizing the transition from circular to elliptic crater formation. a) Transition regime. b) Ricochet regime. c) Grazing regime. The figures on the left side are from the early stage of crater formation. Tracers show peak pressures and those belonging to the projectile are framed with a white dashed line. Images on the right side show the corresponding craters at a late stage. Projectile material has been removed in post-processing, to obtain insights in the "real" crater structure.

A consistent concept for crater formation: Based on the results presented, we propose a concept for crater formation that is applicable for arbitrary impact angles. This concept combines the approach of a static point source [11,12] and the model of a moving point source [13].

In its beginning, crater formation is controlled by the momentum of the projectile. Thus, some energy is released along the trajectory which explains the initial formation of elliptical craters even at moderate oblique impact angle. While penetrating into the target, once the projectile approaches a certain depth, the so-called *depth of burial* [9], the remaining energy is released nearly instantaneously (accordant to the point-source concept). This results in a highly symmetric excavation flow promoting a circular crater shape. With decreasing impact angle the depth of burial is shifted towards the target surface and, thus, a smaller amount of the initial energy is available for the circular excavation flow.

Conclusion: The general shape of the crater is the result of a complex interaction between the asymmetric excavation flow in the beginning (moving point source) and a symmetric flow (point source) later on. For a precise mathematical description of crater formation further studies are intended to quantify the influence of the impact angle, impact energy, and material strength on the depth of burial.

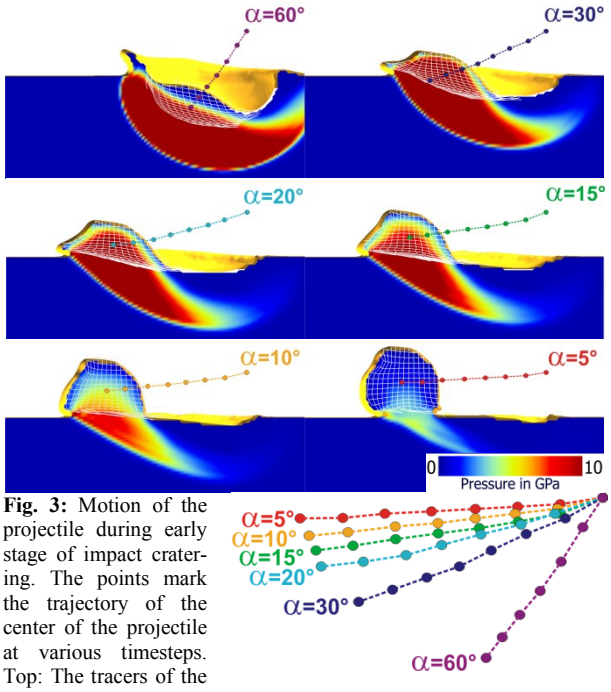

Fig. 3: Motion of the projectile during early stage of impact cratering. The points mark the trajectory of the center of the projectile at various timesteps. Top: The tracers of the projectile are connected to a mesh which allows visualizing the deformations. Right: Projectile motion for the impact angles in a direct comparison.

Acknowledgments: This work was funded by the Helmholtz-Alliance HA-203 / "Planetary Evolution and Life" by the Helmholtz-Gemeinschaft Deutscher Forschungszentren (HGF).

References: [1] Bottke, W.F. Jr., Love, S.G., Tytell, D., and Glotch, T., Icarus, Vol. 145, pp. 108-121, 2000. [2] Elbeshausen D., Wünnemann K., and Collins G.S., Icarus, Vol. 204, pp. 716-731, 1009. [3] Elbeshausen D. and Wünnemann K. (2011) *Proc. HVIS XI*, 287-301. [4] Davison T.M. et al. (2011) *Meteoritics & Planet. Sci., 46* (10), 1510–1524. [5] Burchell, M.J., Mackay, N.G., J. Geophys. Res., Vol. 103, pp. 22761-22774, 1998. [6] Collins G.S.et al. (2011). *Earth Planet. Sci. Letters, 310*. [7] Collins, G.S., Davison, T., Elbeshausen, D., and Wünnemann, K., LPSC XL, Abstract #1620, 2009. [8] Tillotson, J.H., Report GA-3216, General Atomic, San Diego, CA, 1962. [9] Melosh, H.J., Impact Cratering: A Geologic Process. Oxford Univ. Clarendon, Oxford, 1989. [10] Schultz P.H. and Wrobel K.E. (2012). *J. Geophys. Res. Letters, 117*(E4). [11] Holsapple K.A. and Schmidt R.M. (1982). *J. Geophys. Res., 87*(B3), 1849–1870. [12] Papadopoulos M. (1963). *Proc. Royal Soc. London, 273*(1353), 198–221. [13] Anderson J.L.B. and Schultz P.H. (2006). *Int. J. Imp. Engin., 33*(1-12), 35–44.